Growth rate dependent trap density in polythiophene-fullerene solar cells and its implications

Kanwar S. Nalwa,[1] Rakesh C. Mahadevapuram,[2] and Sumit Chaudhary[1,2,a)]
[1]*Department of Electrical and Computer Engineering, Iowa State University, Ames, Iowa 50011, USA*
[2]*Department of Material Science and Engineering, Iowa State University, Ames, Iowa 50011, USA*

(Received 28 September 2010; accepted 10 February 2011; published online 4 March 2011)

To understand the effect of processing conditions such as spin coating speed and drying rate on the density of defects; poly(3-hexylthiophene):fullerene-derivative solar cells A, B, and C were fabricated with solvent drying times of ~40 min, 7 min, and 1 min, respectively. We show that slowest grown device A has one order of magnitude less subband gap traps than device C. The open circuit voltage and its light intensity dependence was strongly affected by interfacial recombination of carriers at subgap defect states. The losses due to trap-assisted recombination can even dominate over bimolecular recombination, depending on the density of defect states © *2011 American Institute of Physics*. [doi:10.1063/1.3560483]

Organic photovoltaics (OPVs) have gained much attention in the past two decades because they offer the promise of low-cost solar-electric conversion, with advantages including mechanical flexibility, light weight, ease of processing and roll-to-roll production capability. Significant progress has been made over the past five years through optimization of materials processing parameters[1–3] and the emergence of new conjugated polymers with tailored energy levels.[4–6] Power conversion efficiency >7% has recently been achieved.[5] Yet, the field of OPVs seems to be progressing almost more by trial and error than by conception, ascribing to the lack of fundamental understanding about several aspects, e.g., defects. In order to further improve OPV performance, it is crucial to extract information about defect states and their role as trapping or recombination centers.

Defects often have a controlling influence on the properties of inorganic semiconductors,[7] yet their role in OPVs remains mostly overlooked, let alone the factors that give rise to these defects. Semiconductor properties such as charge carrier mobility, exciton diffusion length, and photostability of conjugated polymers have been shown to be strongly influenced by mid gap states arising from defects.[8,9] Defects within the band gap alter the electric field profile and might reduce the drift driving force for the charge transport, and consequently diminish carrier collection at the contacts.[10] Depending upon the amount of defects and their recombination strength, the losses due to trap-assisted recombination can lower the fill factor and short-circuit current. This was shown for the case of trap-limited electron transport in bulk heterojunction (BHJ) OPV cells with cyano-poly(phenylenevinylene) (PPV) derivatives as electron acceptors.[11,12] When defect states are present in the electron donor, the dissociation of bound pairs at the interface leads to free carriers, but now part of the holes can be trapped. For the holes trapped close to the interface, there is a probability of recombination with the free electrons in acceptor, leading to loss of both carriers. This trap-assisted recombination process adds to the Langevin (bimolecular) recombination, contributing to loss mechanisms in a BHJ OPV. Therefore, it becomes imperative to understand the processing-related factors that produce these defects to be able to defect-engineer the OPVs for achieving higher performance.

Processing factors such as thermal annealing and slow growth have been shown to increase hole mobility, polymer crystallization, photon absorption, and hence, the efficiency of the OPVs.[6,7] But the effect of growth conditions on the defect density is not quantitatively known. This paper investigates the effect of growth rate on the defects in poly(3-hexylthiophene): [6,6]-phenyl-C61-butyric acid methyl ester (P3HT:PCBM) based BHJ PV cells and their influence on the electrical properties of the OPV cells. Energy distributions [density-of-states (DOS)] of defects in the effective band gap of P3HT:PCBM bulk heterojunctions are determined by analyzing capacitance dependence on both bias voltage $C(V)$ and frequency $C(f)$ of complete cells,[13] as well as subband gap quantum efficiency measurement. This study reveals that slower growth rate leads to reduction in total defect density by an order of magnitude.

For device fabrication, a conducting film of poly(3,4-ethylenedioxythiophene) doped with poly(styrenesulfonate) was spin coated on cleaned ITO glass substrate. Subsequently, P3HT:PCBM (1:1 ratio, total 17 mg/ml in dichlorobenzene) active layers (A, B, and C) were spin coated (under an argon atmosphere) at 400 rpm, 600 rpm, and 1000 rpm for 30 s, 60 s, and 60 s, obtaining solvent evaporation time of ~40 min, 7 min, and 1 min and thicknesses of 350 nm, 220 nm, and 140 nm, respectively. The solvent evaporation time after spin coating was measured by visually inspecting the change in film color when it solidifies from the liquid phase. Al (100 nm) electrode was deposited by thermal evaporation on top of the active layer. The laser wavelength and power used for acquiring Raman spectra was 488 nm and 0.23 mW, respectively. To measure photocurrent versus voltage, devices were illuminated using ELH quartzline lamp operating at 1 sun intensity, i.e., 100 mW/cm^2 (calibrated using crystalline Si photodiode with a KG-5 filter). Intensity dependence of the open circuit voltage (V_{oc}) was measured using a set of neutral density filters. Subgap external quantum efficiency (EQE) measurements were done using ELH Quartzline lamp and a monochromator with a lock-in amplifier to eliminate background noise. For hole

a)Electronic mail: sumitc@iastate.edu.

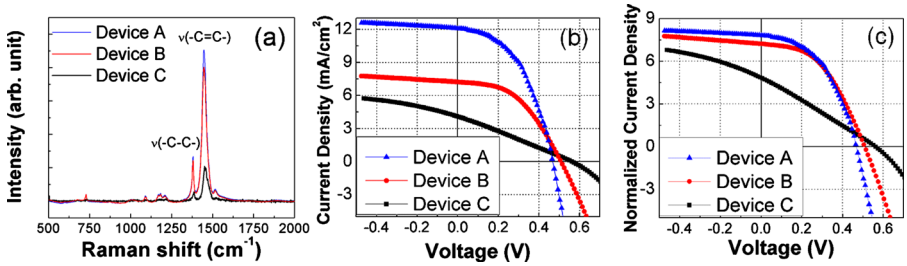

FIG. 1. (Color online) (a) Raman spectra of the active layer and (b) photocurrent J_L-V characteristics under illumination for three device types with different spin coating conditions. (c) Photocurrents, J_L of devices A and C have been normalized, such that the devices have optical absorption equivalent to device B, thus, eliminating the optical absorption variations due to different thicknesses.

mobility measurements, Pd was used as the top electrode to ensure hole only transport, and electric field dependence of hole mobility was taken into account. Zero field hole mobilities were calculated by fitting the linear region (at high voltage) of $\log(J/V^2)$ versus $V^{1/2}$ (where J is current density) plots obtained in dark. At high electric fields, the space charge limited current becomes predominant, such that the effects of traps on the charge transport can be neglected because all the traps are filled.[14] The capacitance measurements were performed with a PARSTAT-2273 equipped with a frequency analyzer module. ac oscillating amplitude was as low as 10 mV (rms) to maintain the linearity of response. Measurements were performed at zero bias for $C(f)$ and at 100 Hz for $C(V)$ analysis, always in dark conditions and at room temperature.

In Fig. 1(a), the Raman spectra show peaks at 1440–1450 and 1380 cm^{-1}, that are attributed to the –C=C– symmetric stretching ($\nu_{C=C}$) and the –C–C– skeletal stretching (ν_{C-C}) of the thiophene ring, respectively.[15–17] When P3HT is more crystalline, the thiophene rings are, on average, more closely stacked. This should lead to narrowing in the $\nu_{C=C}$.[15–18] The values of full width at half maximum for this peak were 29.5 cm^{-1}, 30.25 cm^{-1}, and 32.25 cm^{-1} for device A, B, and C, respectively. The minimum value for device A is another signature of polymer self-organization contributing to increased crystallinity of P3HT. Hence, slow growth (high solvent evaporation time is observed to impart more crystallinity to the P3HT phase in device A as compared with the fast grown device C. As shown in Fig. 1(b), slow-grown device A exhibits short-circuit current density of 12 mA/cm^2 which is one of the highest values reported in literature for this system[1,2] and is ascribed to thicker film (more photons absorbed) as well as more crystalline nature of P3HT (high hole mobility $\sim 8\times10^{-4}$ $cm^2\ V^{-1}\ s^{-1}$). Fast growth clearly increases the V_{oc} of the device C due to increase in the energy of interfacial charge-transfer state as a result of amorphous nature of P3HT.[19] This is accompanied by a decrease in fill factor, from ~50% for device A to 27% for device C. Figure 1(c) illustrates similar information as Fig. 1(b), but the variation in photocurrents due to different thicknesses (different optical absorption) has been eliminated, thus, revealing only the effect of charge transport on photovoltaic performance. Low fill factor in fast grown film has been earlier attributed to a decrease in hole mobility ($\sim 2.0\times10^{-6}$ $cm^2\ V^{-1}\ s^{-1}$) and unbalanced charge transport leading to space charge-limited photocurrent.[1] However, the effect of P3HT morphology and resulting defects remains yet to be identified.

In Fig. 2(a), the subband gap DOS as a function of energy with respect to the P3HT highest occupied molecular orbital (HOMO) level, $E-E_{HOMO}$ for devices A, B, and C is plotted. The plot was generated from $C(V)$ and $C(f)$ measurements, using method detailed by Boix *et al.*[13] The energy density of defect states, $g_t(E_\omega)$ can be analyzed by regarding a Gaussian shape[20] centered at the maximum of the distribution E_0

$$g_t(E_\omega) = \frac{n_t}{\sqrt{2\pi\sigma}}\exp\left[-\frac{(E_0-E_\omega)^2}{2\sigma^2}\right], \tag{1}$$

where E_ω is the demarcation energy and σ is the disorder parameter. n_t, the total density of traps is found to be 3.3×10^{15} cm^{-3}, 5.2×10^{15} cm^{-3}, and 2.1×10^{16} cm^{-3} for devices A, B, and C, respectively. The investigated defect states shown in Fig. 2(a) have been shown to only belong to P3HT, as such behavior was not exhibited at all by devices containing only PCBM molecules.[13] The defect density follows the same trend as that of noncrystallinity (disorder) of P3HT in films, i.e., increasing on increasing the growth rate. These states could be a consequence of conformational defects accompanying the ordering of the aromatic chain backbone. Several types of structural defects such as twisting-tilting of one monomer unit out of the conjugation plan and loss of p-p stacking either through tilting or lateral displacement of ad-

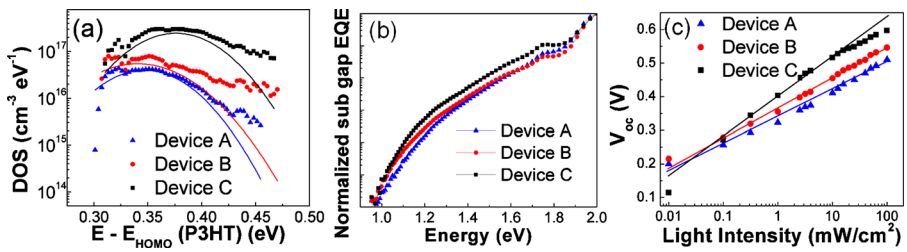

FIG. 2. (Color online) (a) Density of defect states as a function of the energy with respect to the P3HT HOMO level (demarcation energy), $E-E_{HOMO}$, (b) normalized (at 2.0 eV) EQE spectra measured in the subgap region, and (c) V_{oc} light intensity dependence of devices A, B, and C. The solid lines in (c) are linear fits used to calculate the slope, S.

jacent polymer chains have been known to create defect states in the P3HT HOMO-lowest unoccupied molecular orbital (LUMO) gap.[21,22] The extent of such structural distortions is related to the crystallinity of the film, since disorder (twisting and coiling of P3HT chains) increases with increase in amorphous nature.[1] Therefore, slow growth can be directly linked to higher crystallinity and lower subgap defect density of P3HT in film A. Normalized (at 2.0 eV) EQE spectra of OPVs in the subgap region is shown in Fig. 2(b). Lower subband gap absorption in device A further corroborates the aforementioned finding that slow growth induced self-organization leads to lower defect density in the P3HT band gap.

In case of Langevin (bimolecular) recombination of free carriers being the only loss mechanism, it has been shown that the V_{oc} of the OPVs follow[23]

$$V_{oc} = \frac{E_{gap}}{q} - \frac{kT}{q}\ln\left[\frac{(1-P)\gamma N_c^2}{PG}\right],$$

where E_{gap} is the energy difference between the HOMO of the electron donor and the LUMO of the electron acceptor, q is the elementary charge, k the Boltzmann constant, T the temperature, P is the dissociation probability of the electron-hole pairs into free carriers, γ is the recombination constant, N_c is the density of states in the conduction band, and G is the generation rate of electron-hole pairs. Since G is the only term directly proportional with the light intensity (with P and γ not depending on it), this formula contains the dependence of the V_{oc} on the light intensity. Therefore, the slope $S=(kT/q)$ of the V_{oc} versus the natural logarithm of the light intensity is predicted by the formula and has been found to be in good agreement for MDMO-PPV=Poly(2-methoxy-5-(3′-7′-dimethyloctyloxy)-1,4–phenylenevinylene)-PPV:PCBM solar cells.[23] A slope of $1.5(kT/q)$ has been measured for all-polymer solar cells with electron traps contained in the acceptor phase.[11,12] This deviation has been explained by including trap-assisted Schokley–Read–Hall recombination at the electron donor-acceptor interface in the device model developed for BHJ solar cells.[11,12,24] The trap-assisted interfacial recombination competes with the Langevin one, thereby, the slope of V_{oc} versus natural logarithm of the light intensity increases with the strength of the trap-assisted recombination. In Fig. 2(c), the dependence of V_{oc} on the light intensity is shown for devices A, B, and C, with $S=1.1$, 1.4, and 1.9 times (kT/q), respectively (calculated from the linear fit). In fast grown film case (device C), with one order of magnitude higher trap density in P3HT than slow grown active layer A, it is expected that the trap-limited recombination is stronger. Consequently, the dependence of V_{oc} on light intensity is more enhanced. The faster decay of V_{oc} for the trap-limited fast grown device C is a direct outcome of the fact that the presence of holes in trap levels above the HOMO of the P3HT raises the hole quasi-Fermi level. This increased amount of trap-assisted recombination in device C also leads to the observed reduction in the fill factor. Furthermore, the additional loss of free carriers due to stronger recombination (along with lower absorption in thinner film) results in reduction in the photocurrent in device C.

In conclusion, the slow growth assists the formation of self-organized ordered structure in the P3HT/PCBM blend system diminishing morphological defects in P3HT chains. Fast growth, however, results in an order of magnitude higher trap density owing to the structural defects (twists and bends) in P3HT chains. Lowering of hole mobility in fast grown film is expected to promote Langevin recombination, as it increases the hole density due to unbalanced charge transport. On the other hand, trap-assisted interfacial recombination is aggravated by the presence of high trap density. The dependence of open circuit voltage on the light intensity reveals that trap-assisted recombination can possibly dominate over the Langevin recombination at 1 sun condition for films with high enough trap density. However, the quantification of recombination rates is required to determine the actual role of trap-assisted recombination at 1 sun condition and is a topic of our immediate research.

The authors thank state of Iowa's Office of Energy Independence for supporting this work through Iowa Power fund.

[1]G. Li, V. Shrotriya, J. S. Huang, Y. Yao, T. Moriarty, K. Emery, and Y. Yang, Nature Mater. **4**, 864 (2005).
[2]W. L. Ma, C. Y. Yang, X. Gong, K. Lee, and A. J. Heeger, Adv. Funct. Mater. **15**, 1617 (2005).
[3]J. Peet, J. Y. Kim, N. E. Coates, W. L. Ma, D. Moses, A. J. Heeger, and G. C. Bazan, Nature Mater. **6**, 497 (2007).
[4]H. Y. Chen, J. H. Hou, S. Q. Zhang, Y. Y. Liang, G. W. Yang, Y. Yang, L. P. Yu, Y. Wu, and G. Li, Nat. Photonics **3**, 649 (2009).
[5]Y. Y. Liang, Z. Xu, J. B. Xia, S. T. Tsai, Y. Wu, G. Li, C. Ray, and L. P. Yu, Adv. Mater. (Weinheim, Ger.) **22**, E135 (2010).
[6]S. H. Park, A. Roy, S. Beaupre, S. Cho, N. Coates, J. S. Moon, D. Moses, M. Leclerc, K. Lee, and A. J. Heeger, Nat. Photonics **3**, 297 (2009).
[7]P. T. Landsberg, *Recombination in Semiconductors* (Cambridge University Press, Cambridge, 1991).
[8]B. A. Gregg, J. Phys. Chem. C **113**, 5899 (2009).
[9]Z. Q. Liang, A. Nardes, D. Wang, J. J. Berry, and B. A. Gregg, Chem. Mater. **21**, 4914 (2009).
[10]J. Nelson, *The Physics of Solar Cells* (Imperial College Press, London, 2003).
[11]M. M. Mandoc, F. B. Kooistra, J. C. Hummelen, B. d. Boer, and P. W. M. Blom, Appl. Phys. Lett. **91**, 263505 (2007).
[12]M. M. Mandoc, W. Veurman, L. J. A. Koster, B. de Boer, and P. W. M. Blom, Adv. Funct. Mater. **17**, 2167 (2007).
[13]P. P. Boix, G. Garcia-Belmonte, U. Munecas, M. Neophytou, C. Waldauf, and R. Pacios, Appl. Phys. Lett. **95**, 233302 (2009).
[14]M. Giulianini, E. R. Waclawik, J. M. Bell, and N. Motta, Appl. Phys. Lett. **94**, 083302 (2009).
[15]J. Casado, R. G. Hicks, V. Hernandez, D. J. T. Myles, M. C. R. Delgado, and J. T. L. Navarrete, J. Chem. Phys. **118**, 1912 (2003).
[16]P. S. O. Patrício, H. D. R. Calado, F. A. C. de Oliveira, A. Righi, B. R. A. Neves, G. G. Silva, and L. A. Cury, J. Phys.: Condens. Matter **18**, 7529 (2006).
[17]E. Klimov, W. Li, X. Yang, G. G. Hoffmann, and J. Loos, Macromolecules **39**, 4493 (2006).
[18]J. J. Yun, J. Peet, N. S. Cho, G. C. Bazan, S. J. Lee, and M. Moskovits, Appl. Phys. Lett. **92**, 251912 (2008).
[19]K. Vandewal, W. D. Oosterbaan, S. Bertho, V. Vrindts, A. Gadisa, L. Lutsen, D. Vanderzande, and J. V. Manca, Appl. Phys. Lett. **95**, 123303 (2009).
[20]H. Bässler, Phys. Status Solidi B **175**, 15 (1993).
[21]D. Q. Feng, A. N. Caruso, Y. B. Losovyj, D. L. Shulz, and P. A. Dowben, Polym. Eng. Sci. **47**, 1359 (2007).
[22]A. N. Caruso, D. Q. Feng, Y. B. Losovyj, D. L. Schulz, S. Balaz, L. G. Rosa, A. Sokolov, B. Doudin, and P. A. Dowben, Phys. Status Solidi B **243**, 1321 (2006).
[23]L. J. A. Koster, V. D. Mihailetchi, R. Ramaker, and P. W. M. Blom, Appl. Phys. Lett. **86**, 123509 (2005).
[24]L. J. A. Koster, E. C. P. Smits, V. D. Mihailetchi, and P. W. M. Blom, Phys. Rev. B **72**, 085205 (2005).